

Fig. 4.28 Side view flow photos taken at the cross plane  $\theta = 0^\circ$  &  $180^\circ$  for various Rayleigh numbers at  $Q_j = 1.0 \text{ slpm}$  and  $Re_\Omega = 2,335$  ( $\Omega = 30 \text{ rpm}$ ) for (a)  $D_j = 10.0 \text{ mm}$  &  $Re_j = 135$  and (b)  $D_j = 22.1 \text{ mm}$  &  $Re_j = 61$ .

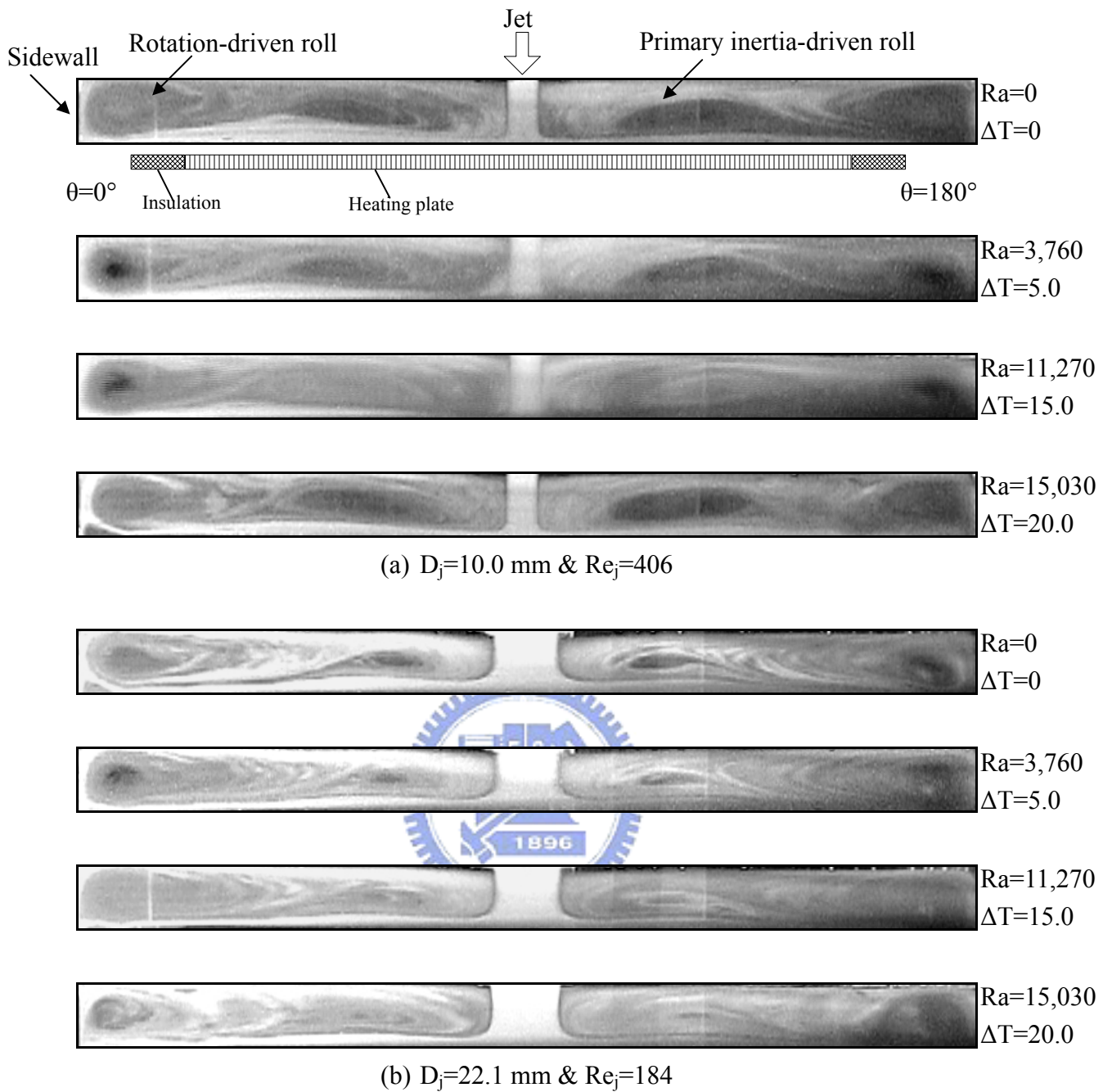
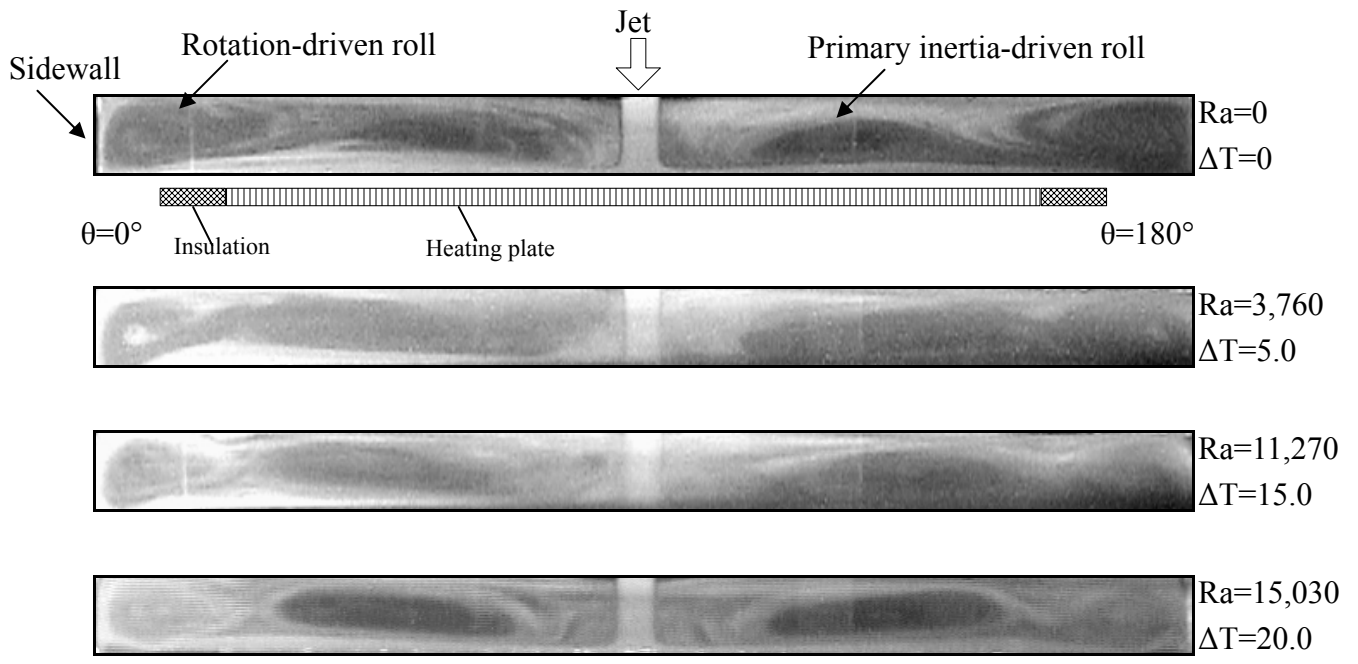
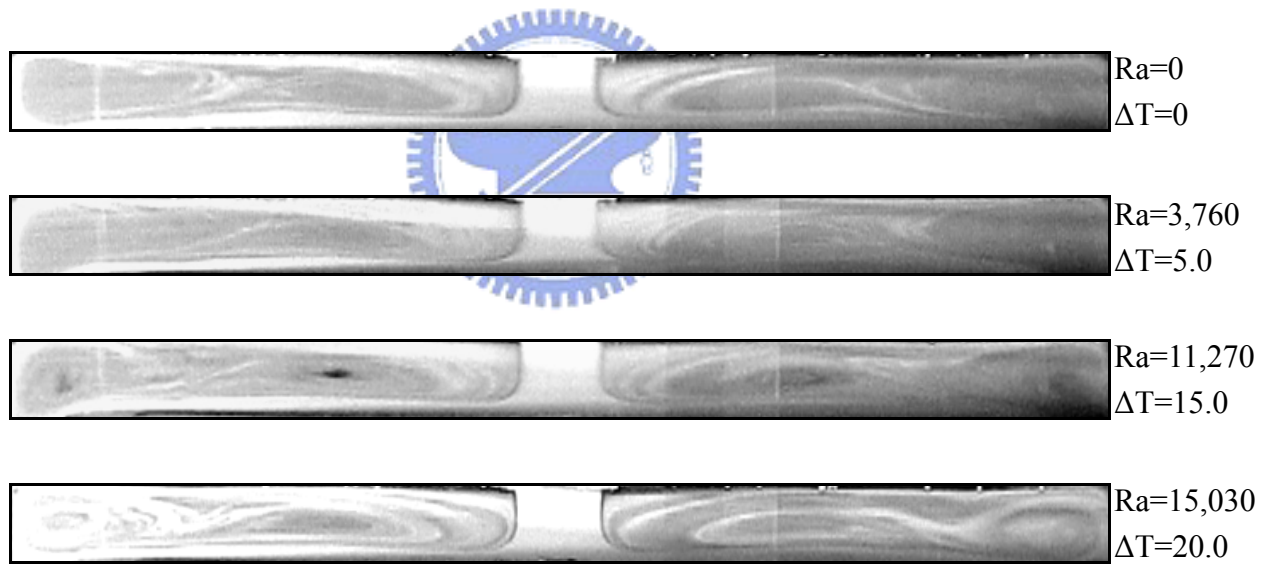


Fig. 4.29 Side view flow photos taken at the cross plane  $\theta = 0^\circ$  &  $180^\circ$  for various Rayleigh numbers at  $Q_j = 3.0 \text{ slpm}$  and  $Re_\Omega = 2,335$  ( $\Omega = 30 \text{ rpm}$ ) for (a)  $D_j = 10.0 \text{ mm}$  &  $Re_j = 406$  and (b)  $D_j = 22.1 \text{ mm}$  &  $Re_j = 184$ .



(a)  $D_j=10.0$  mm &  $Re_j=676$



(b)  $D_j=22.1$  mm &  $Re_j=306$

Fig. 4.30 Side view flow photos taken at the cross plane  $\theta = 0^\circ$  &  $180^\circ$  for various Rayleigh numbers at  $Q_j = 5.0$  slpm and  $Re_\Omega = 2,335$  ( $\Omega = 30$  rpm) for (a)  $D_j = 10.0$  mm &  $Re_j = 676$  and (b)  $D_j = 22.1$  mm &  $Re_j = 306$ .

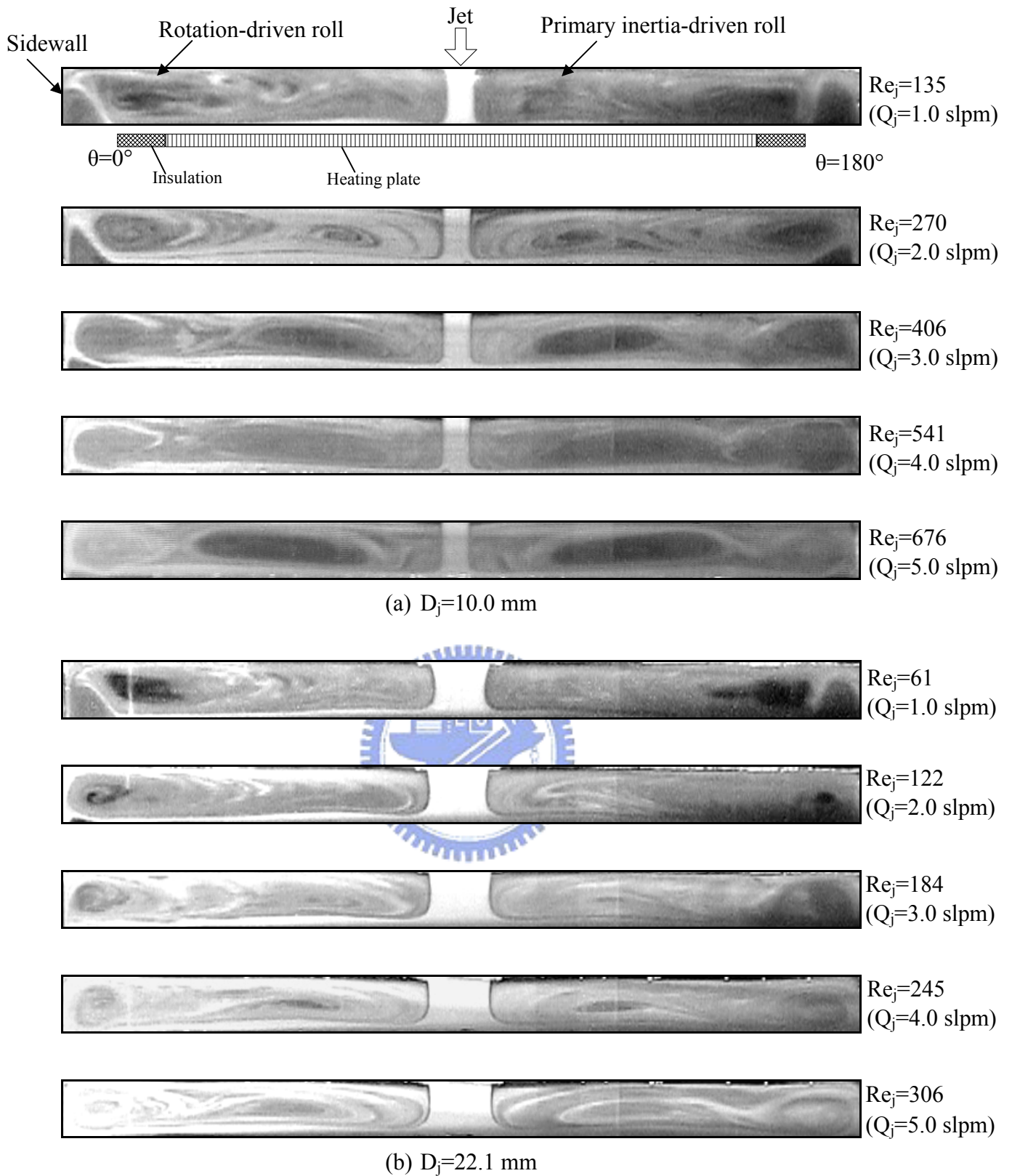


Fig. 4.31 Steady side view flow photos taken at the cross plane  $\theta = 0^\circ$  &  $180^\circ$  for various jet Reynolds numbers at  $Ra = 15,030$  ( $\Delta T = 20.0$  ) and  $Re_\Omega = 2,335$  ( $\Omega = 30$  rpm) for  $D_j =$  (a) 10.0 mm and (b) 22.1 mm.

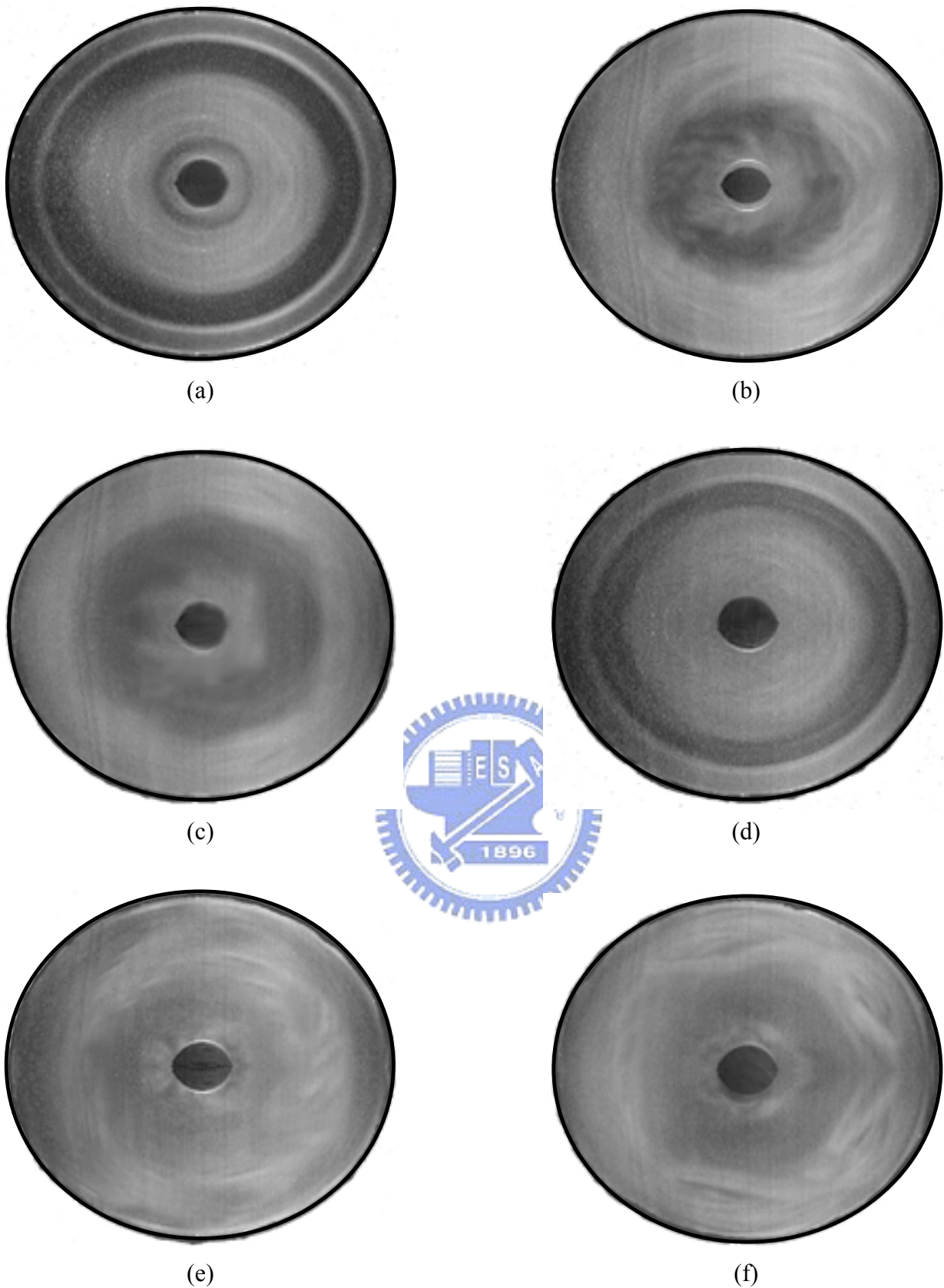
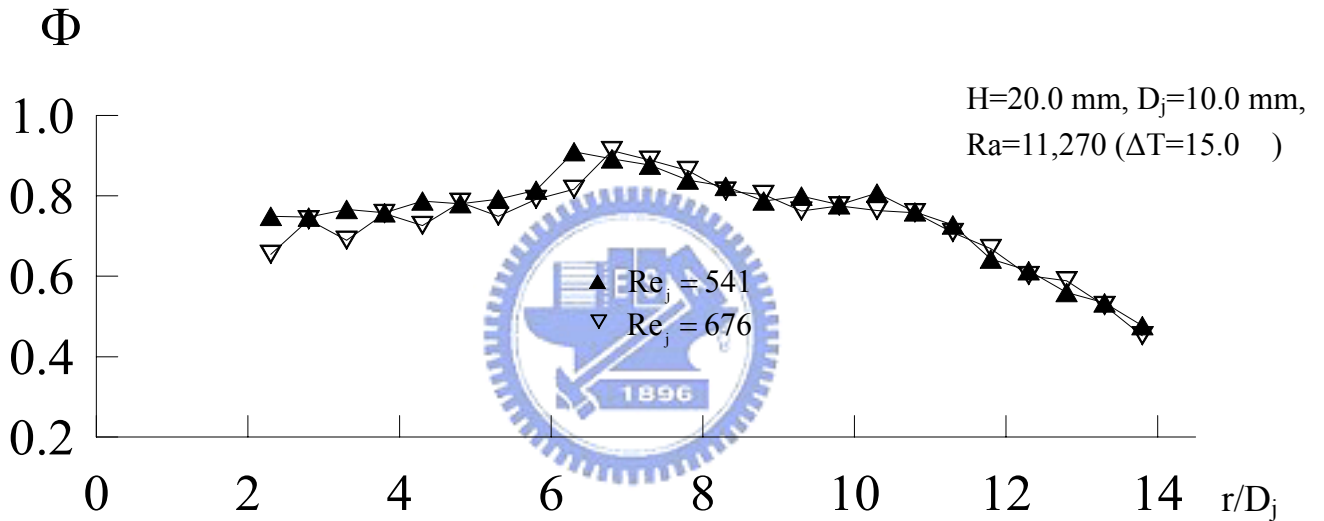
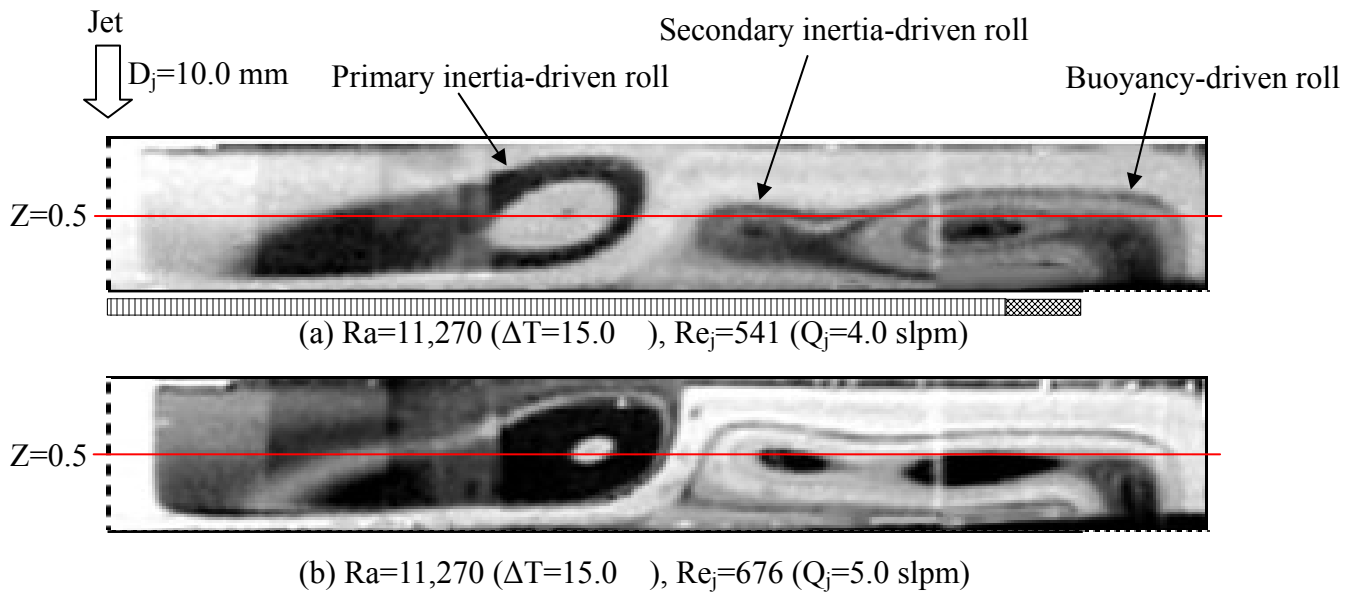


Fig. 4.32 Steady top view flow photos taken at the middle horizontal plane between the disk and chamber top with  $Ra = 15,030$  ( $\Delta T = 20.0$  ) and  $Re_{\Omega} = 2,335$  ( $\Omega = 30$  rpm) for  $D_j = 10$  mm at  $Re_j =$  (a) 135, (b) 406, and (c) 676 and  $D_j = 22.1$  mm at  $Re_j =$  (d) 61, (e) 184, and (f) 306.





(c) radial variation in non-dimensional steady air temperature

Fig. 4.33 Steady side view flow photos at the cross plane  $\theta=180^\circ$  with  $Re_\Omega=0$  ( $\Omega=0$  rpm),  $Ra=11,270$  ( $\Delta T=15.0$  ),  $H=20.0$  mm, and  $D_j=10.0$  mm at  $Re_j=(a)541$  and (b)676, and (c) the corresponding radial variations of non-dimensional steady air temperature at  $Z=0.5$ .

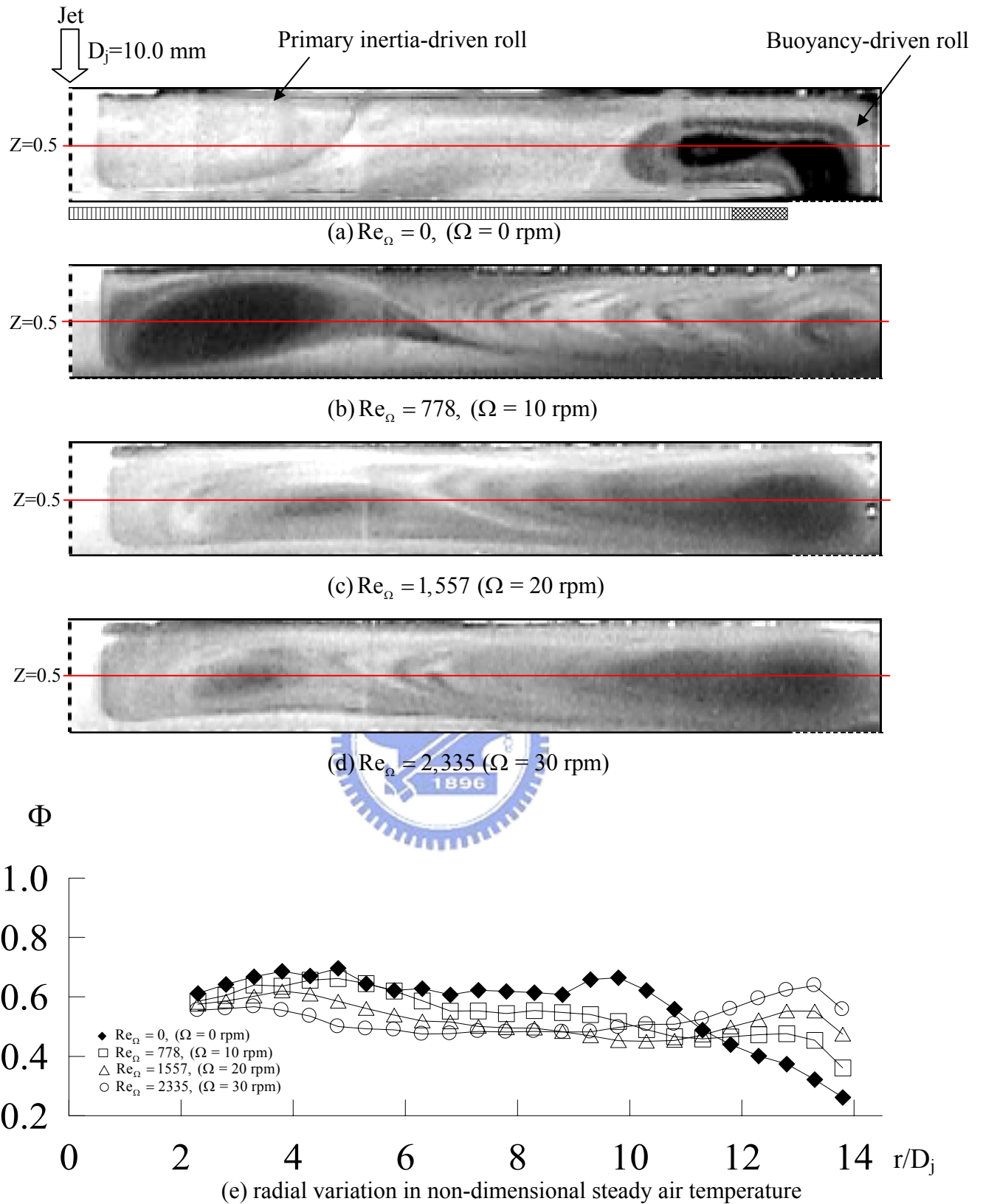


Fig. 4.34 Steady side view flow photos at the cross plane  $\theta = 180^\circ$  with  $Re_j = 135$  ( $Q_j = 1.0$  slpm),  $Ra = 3,760$  ( $\Delta T = 5.0$ ),  $H = 20.0$  mm and  $D_j = 10.0$  mm at  $Re_\Omega =$  (a) 0, (b) 778, (c) 1,557 and (d) 2,335, and (e) the corresponding radial variations of non-dimensional steady air temperature at  $Z = 0.5$ .

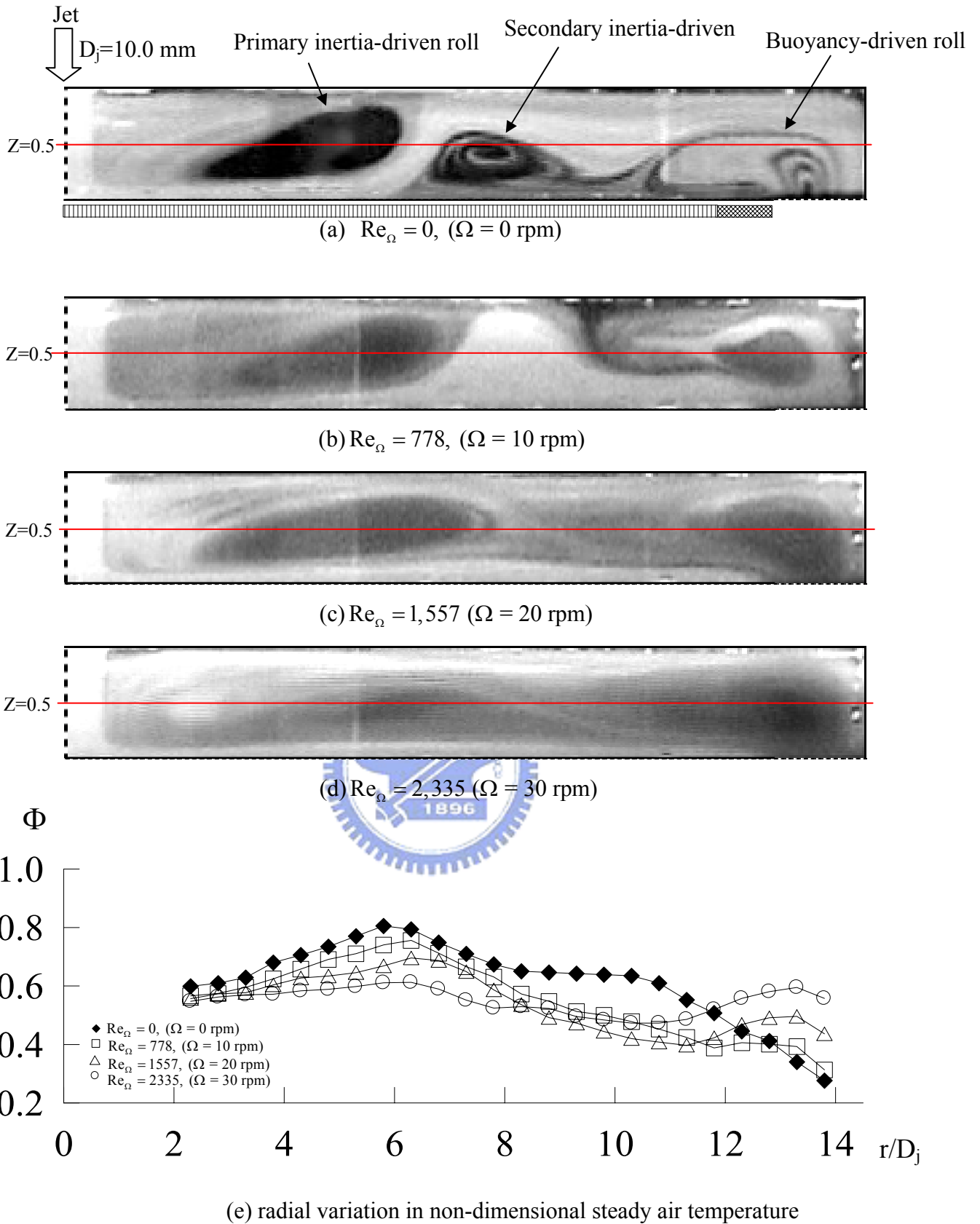


Fig. 4.35 Steady side view flow photos at the cross plane  $\theta = 180^\circ$  with  $\text{Re}_j = 406$  ( $Q_j=3.0$  slpm),  $\text{Ra}=3,760$  ( $\Delta T=5.0$  ),  $H=20.0$  mm, and  $D_j=10.0$  mm at  $\text{Re}_\Omega =$  (a)0, (b)778, (c)1,557, (d)2,335 and (e) the corresponding radial variations of non-dimensional steady air temperature at  $Z=0.5$ .



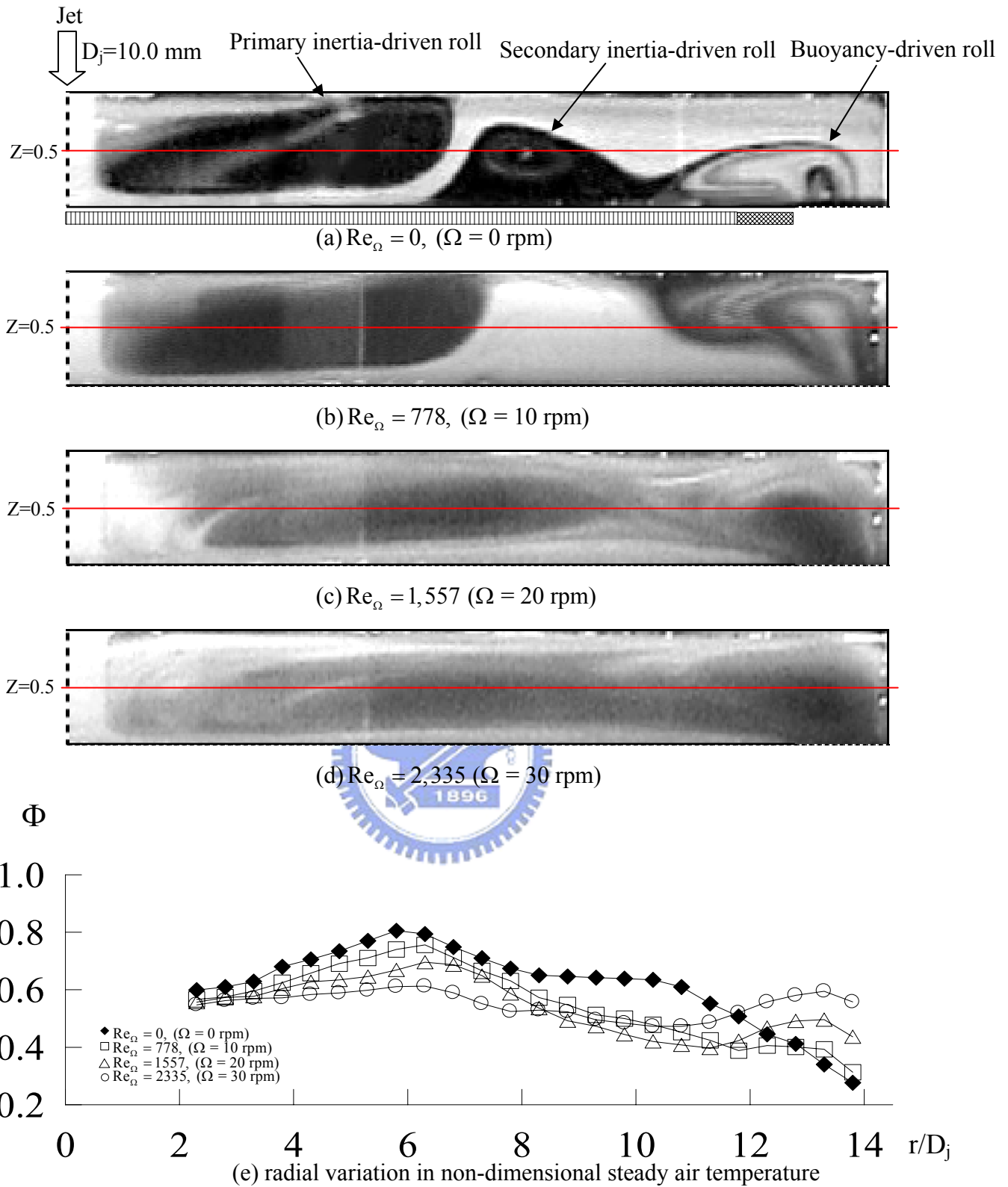
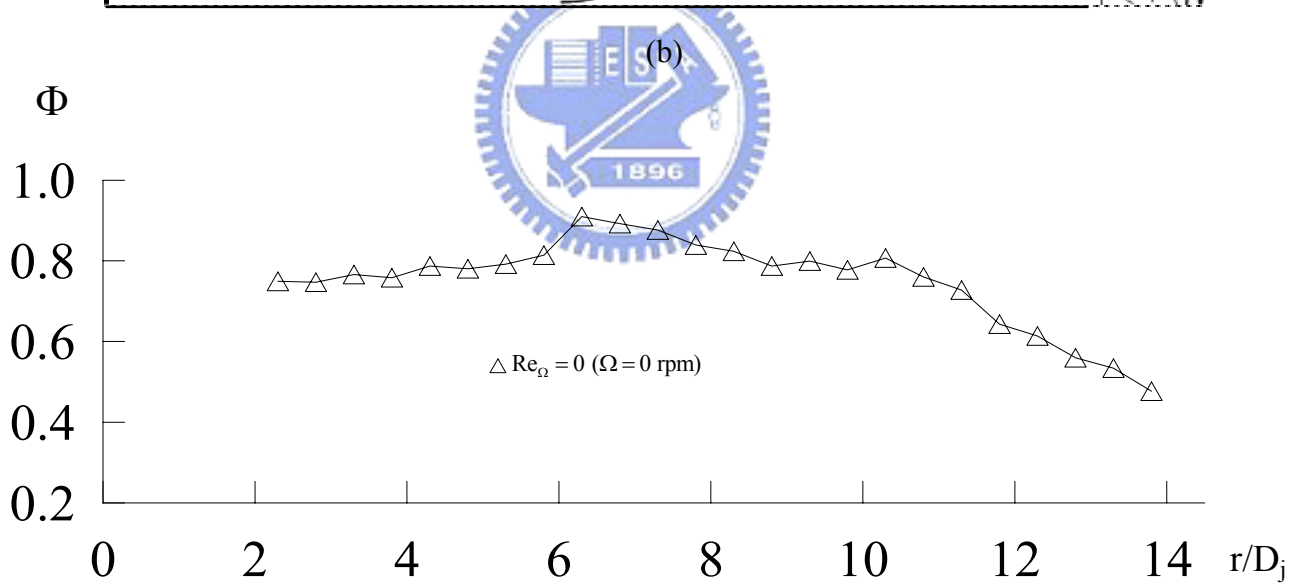
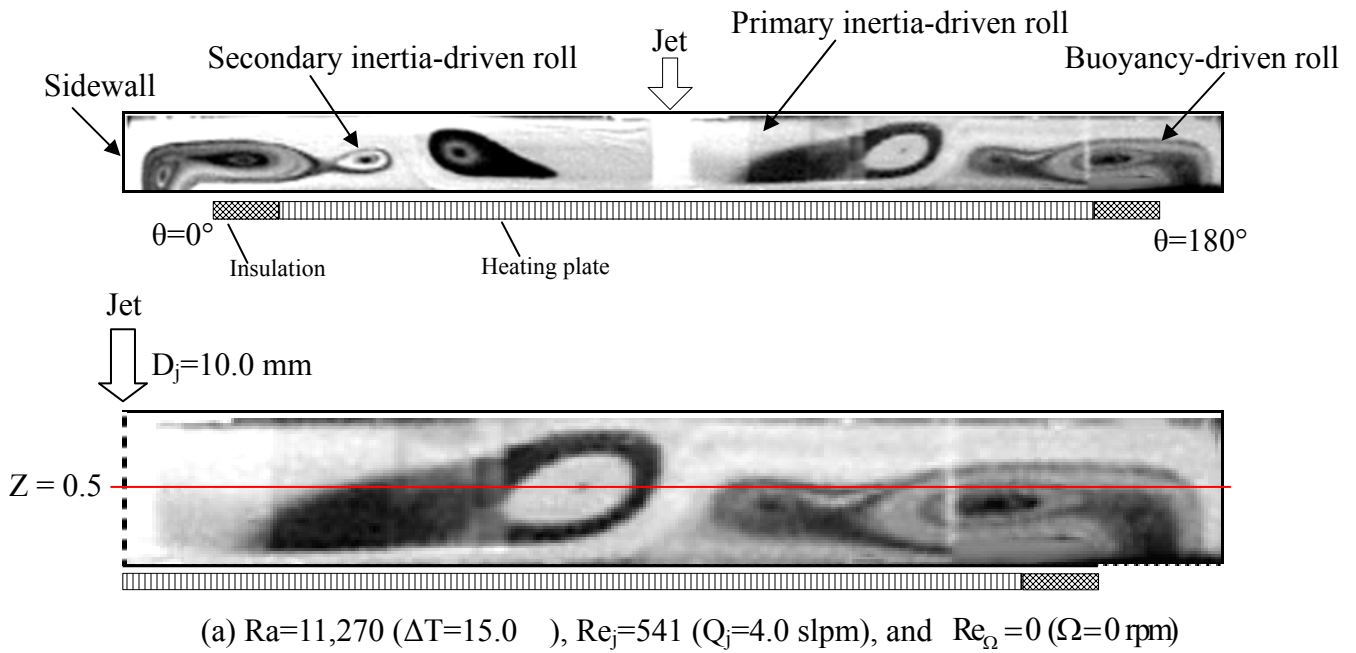


Fig. 4.36 Steady side view flow photos at the cross plane  $\theta = 180^\circ$  with  $Re_j = 541$  ( $Q_j = 5.0$  slpm),  $Ra = 3,760$  ( $\Delta T = 5.0$ ),  $H = 20.0$  mm, and  $D_j = 10.0$  mm at  $Re_\Omega =$  (a)0, (b)778, (c)1,557, and (d)2,335 and (e) the corresponding radial variations of non-dimensional steady air temperature at  $Z = 0.5$ .



(c) radial variation in non-dimensional steady air temperature

Fig. 4.37 Steady side view flow photos at the cross plane  $\theta = 0^\circ$  &  $180^\circ$  with (a)  $Re_j = 541$  ( $Q_j = 4.0$  slpm),  $Ra=11,270$  ( $\Delta T=15.0$  ),  $H=20.0$  mm,  $D_j=10.0$  mm and  $Re_\Omega=0$  ( $\Omega = 0$  rpm), (b) the corresponding schematically sketched cross plane vortex flow at  $\theta = 180^\circ$ , and (c) the radial variation of non-dimensional steady air temperature at  $Z=0.5$ .

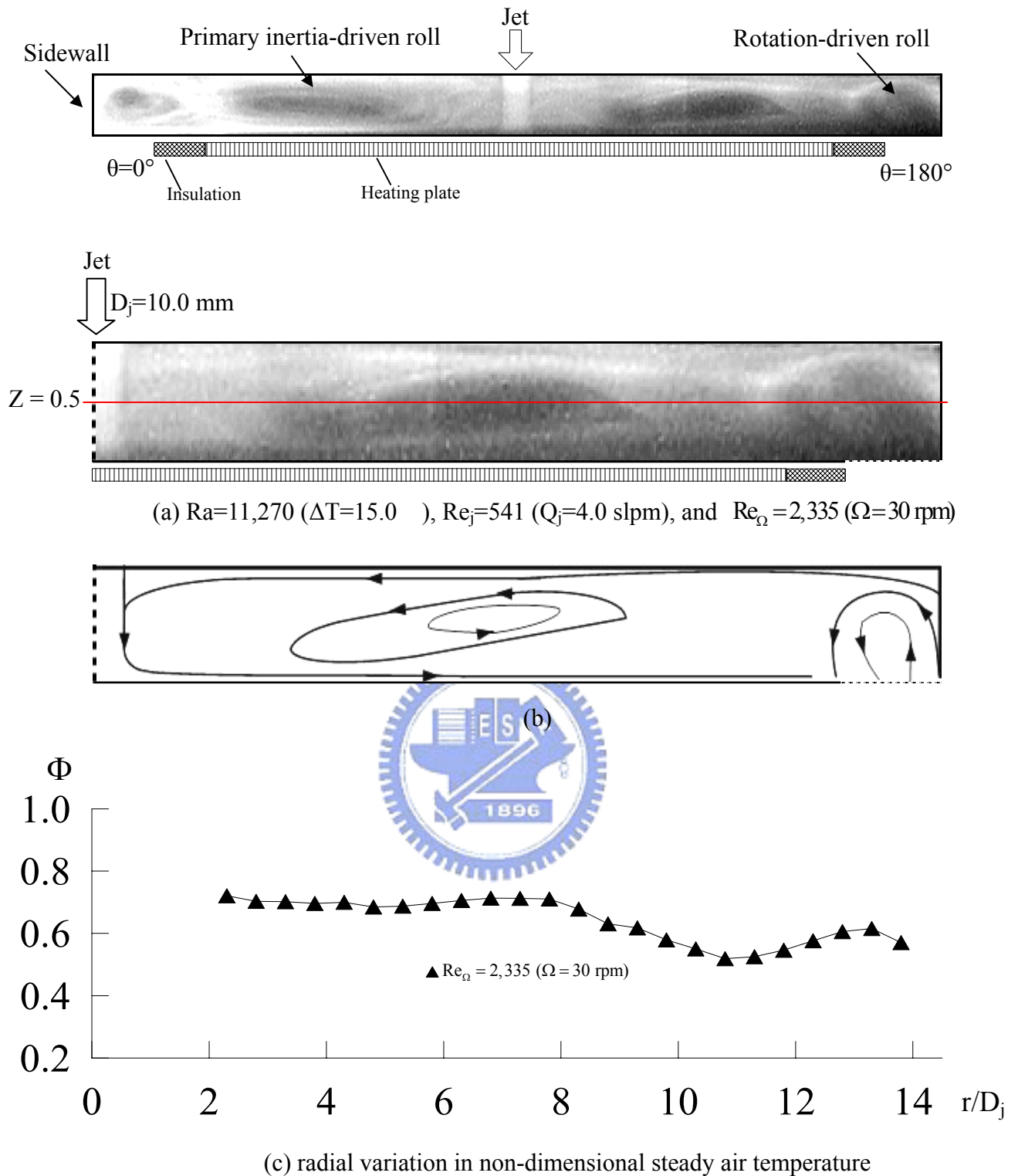
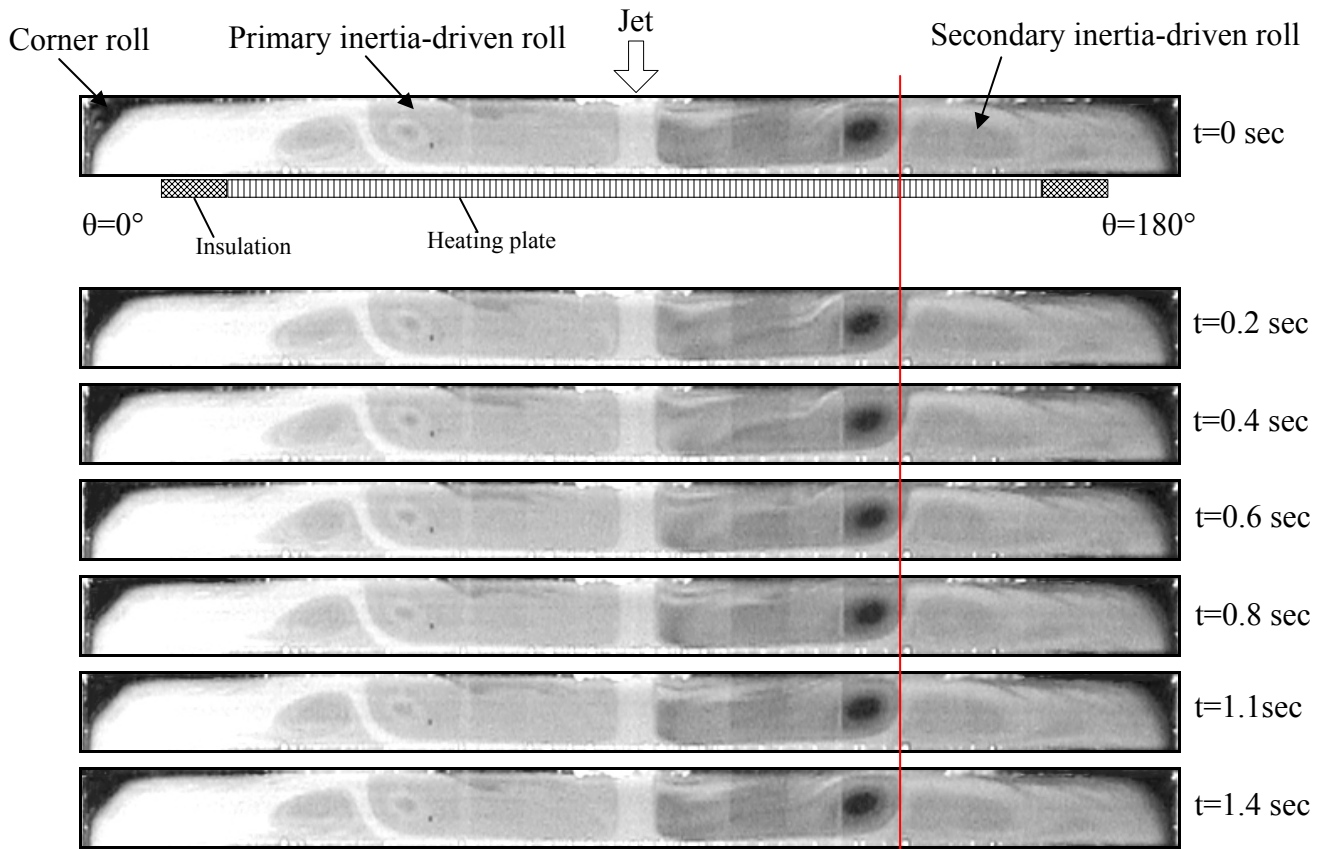
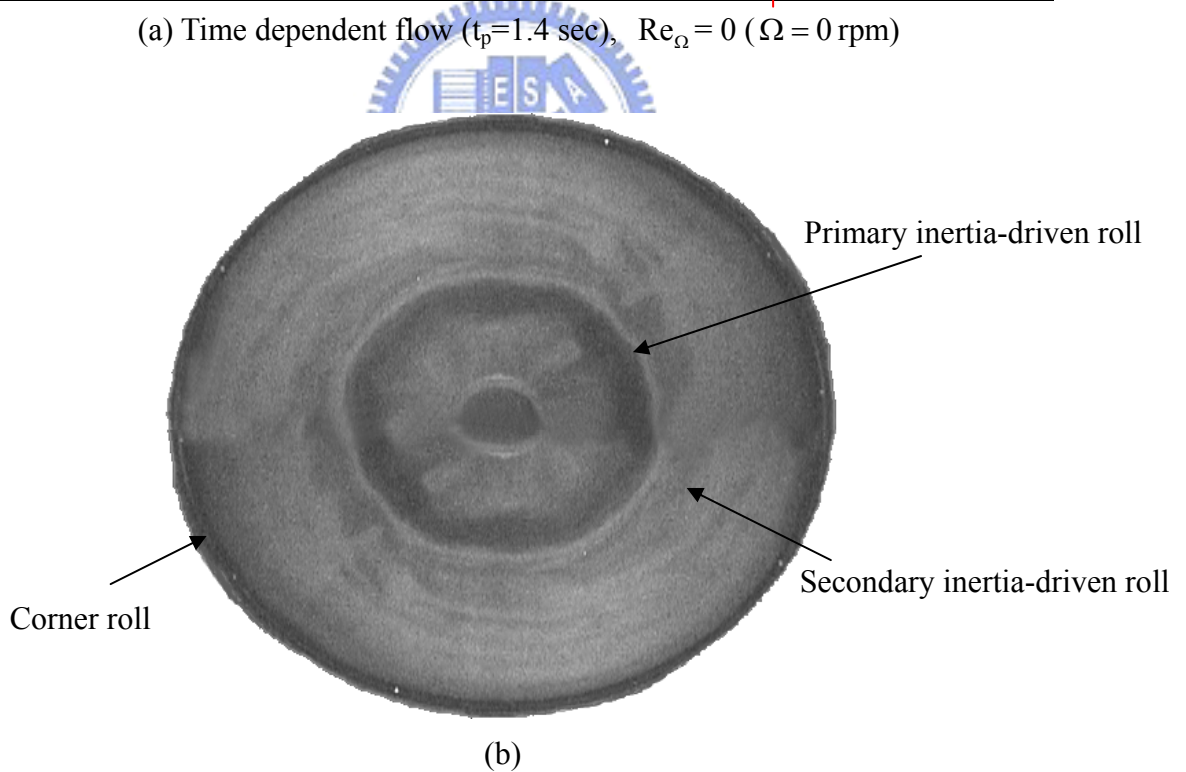


Fig. 4.38 Steady side view flow photos at the cross plane  $\theta = 0^\circ$  &  $180^\circ$  with (a)  $Re_j = 541$  ( $Q_j = 4.0$  slpm),  $Ra=11,270$  ( $\Delta T= 15.0$ ),  $H=20.0$  mm,  $D_j=10.0$  mm and  $Re_\Omega=2,335$  ( $\Omega = 30$  rpm), (b)the corresponding schematically sketched cross plane vortex flow at  $\theta = 180^\circ$  and (c) the radial variation of non-dimensional steady air temperature at  $Z=0.5$ .

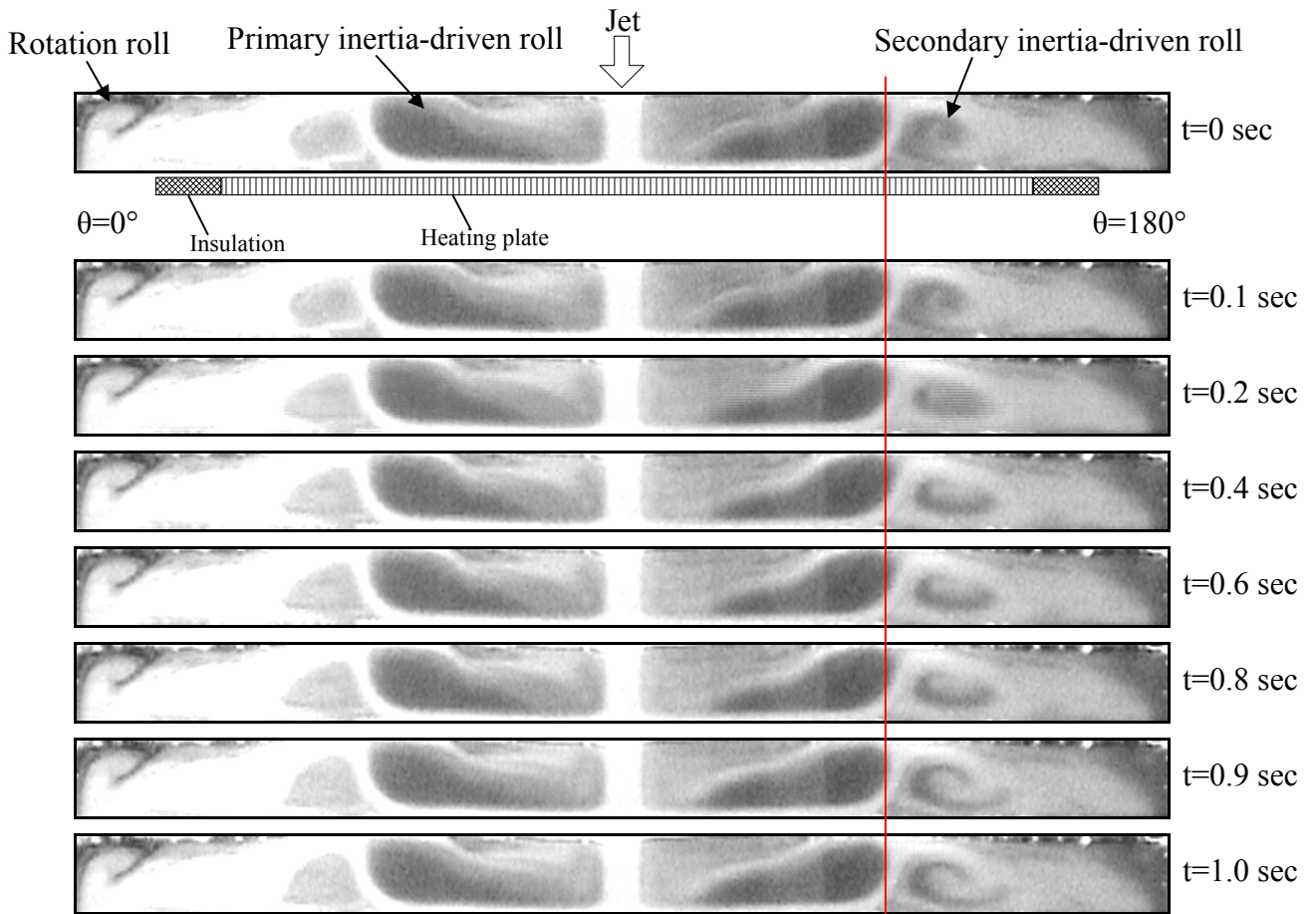


(a) Time dependent flow ( $t_p=1.4$  sec),  $Re_\Omega = 0$  ( $\Omega = 0$  rpm)

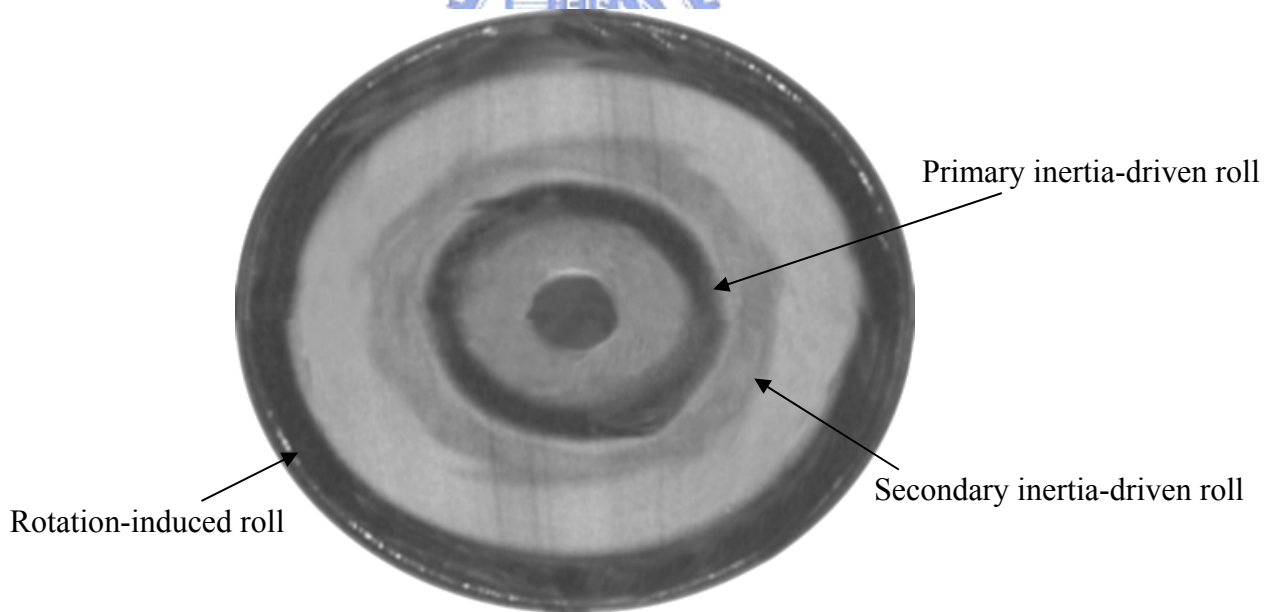


(b)

Fig. 4.39 Time-periodic vortex flow for  $H=20.0$  mm,  $Re_\Omega = 0$  ( $\Omega = 0$  rpm), and  $Ra=0$  ( $\Delta T = 0$ ) at  $Re_j=839$  ( $Q_j=6.2$  slpm) illustrated by (a) side view flow photos taken at the vertical plane  $\theta = 0^\circ$  &  $180^\circ$  at selected time instants in a typical periodic cycle and (b) top view flow photo taken at middle horizontal plane halfway between the injection pipe exit and heated disk at certain time instant in the cycle ( $t_p = 1.4$  sec).



(a) Time dependent flow ( $t_p=1.0$  sec),  $Re_\Omega = 389$  ( $\Omega = 5$  rpm)



(b)

Fig. 4.40 Time-periodic vortex flow for  $H=20.0$  mm,  $Re_\Omega = 389$  ( $\Omega = 5$  rpm), and  $Ra=0$  ( $\Delta T = 0$ ) at  $Re_j = 839$  ( $Q_j=6.2$  slpm) illustrated by (a) side view flow photos taken at the vertical plane  $\theta = 0^\circ$  &  $180^\circ$  at selected time instants in a typical periodic cycle and (b) top view flow photo taken at middle horizontal plane halfway between the injection pipe exit and heated disk at certain time instant in the cycle ( $t_p = 1.0$  sec).



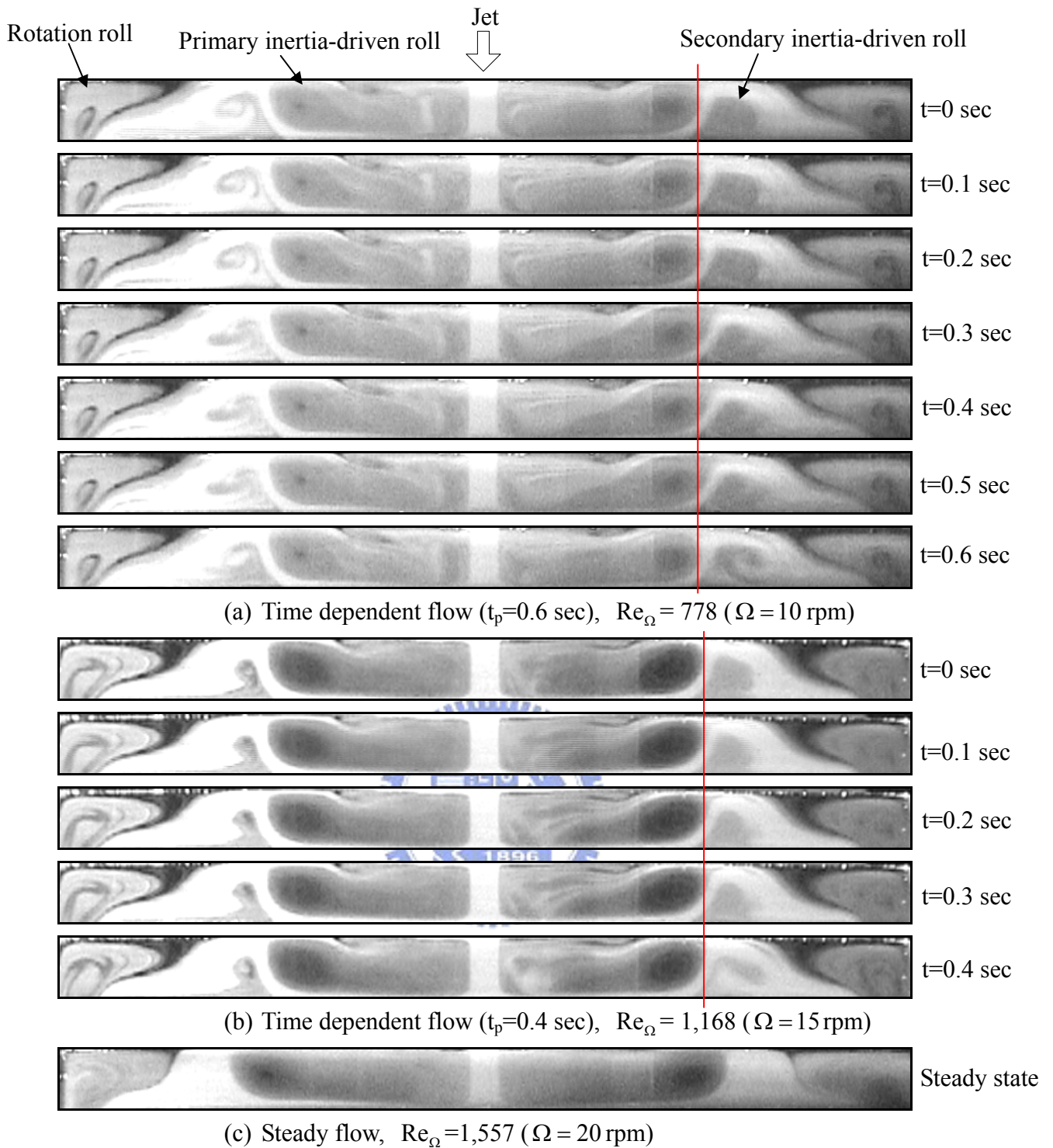


Fig. 4.41 Vortex flows for  $H=20.0$  mm, and  $Ra=0$  ( $\Delta T = 0$ ) at  $Re_j=839$  ( $Q_j=6.2$  slpm) illustrated by side view flow photos taken at the vertical plane  $\theta = 0^\circ$  &  $180^\circ$  at selected time instants in a typical periodic cycle for various rotational Reynolds number: (a)  $Re_{\Omega} = 778$  ( $t_p=0.6$  sec), (b)  $Re_{\Omega} = 1,168$  ( $t_p=0.4$  sec), and (c)  $Re_{\Omega} = 1,557$  (steady state).



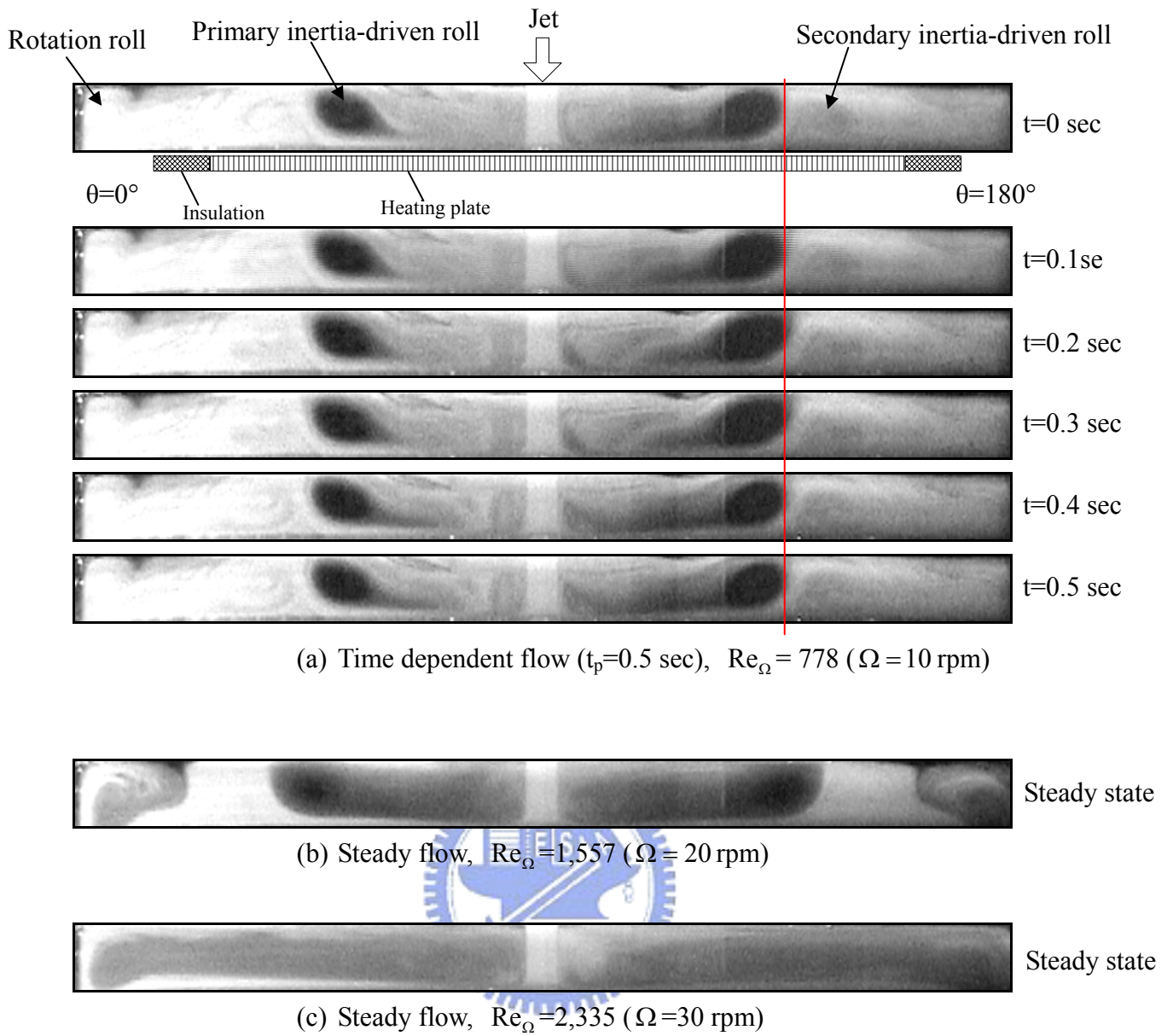


Fig. 4.42 Steady and time-periodic vortex flows for  $H=20.0$  mm and  $Ra=3,760$  ( $\Delta T = 5.0$  ) at  $Re_j=839$  ( $Q_j=6.2$  slpm) for (a)  $Re_\Omega=778$  ( $t_p=0.5$  sec), (b)  $Re_\Omega=1,557$  (steady state), and (c)  $Re_\Omega=2,335$  (steady state).

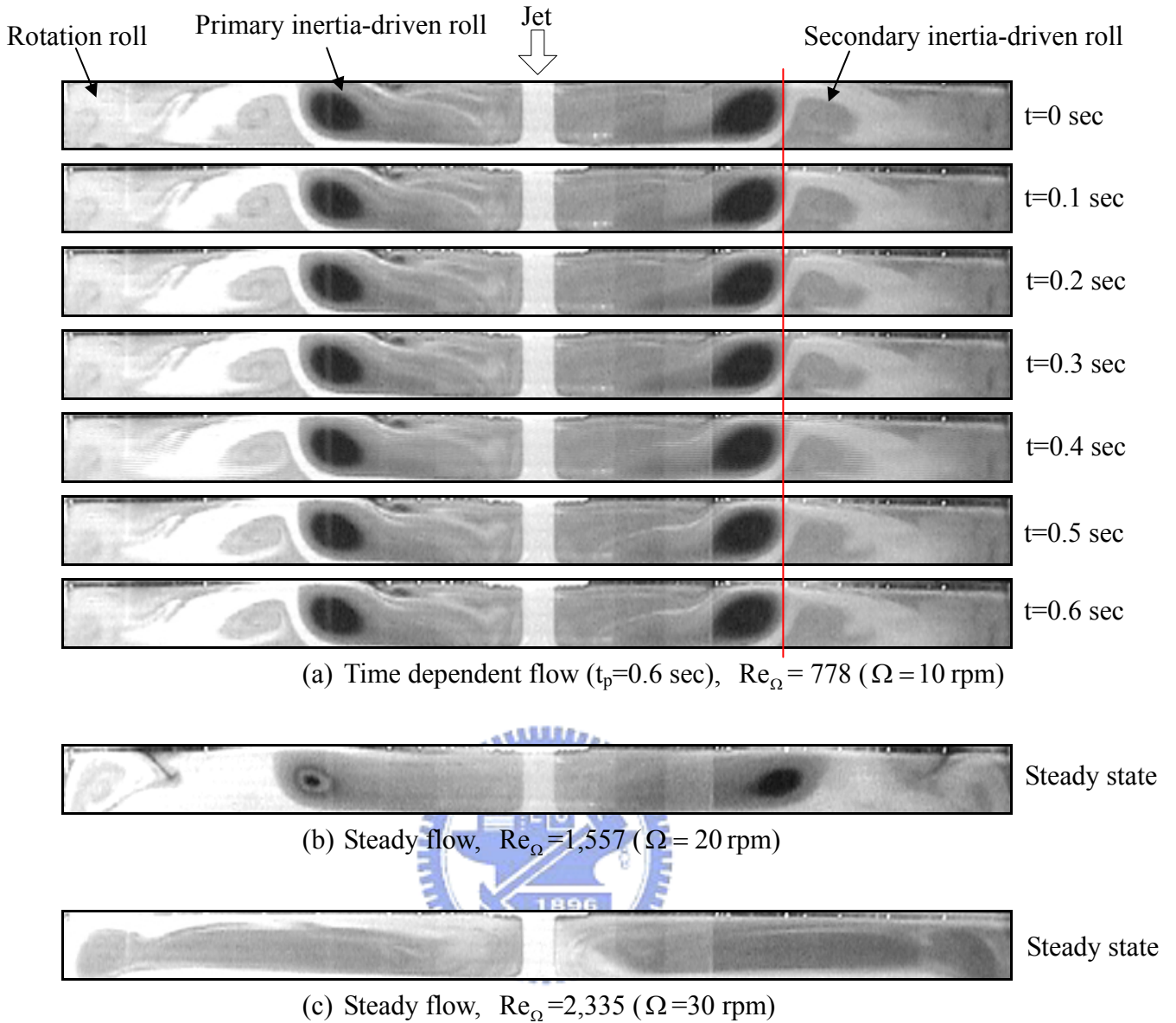


Fig. 4.43 Steady and time-periodic vortex flows for  $H=20.0$  mm and  $Ra=7,520$  ( $\Delta T=10.0$  ) at  $Re_j=893$  ( $Q_j=6.6$  slpm) for (a)  $Re_{\Omega} = 778$  ( $t_p=0.6$  sec), (b)  $Re_{\Omega} = 1,557$  (steady state), and (c)  $Re_{\Omega} = 2,335$  (steady state).

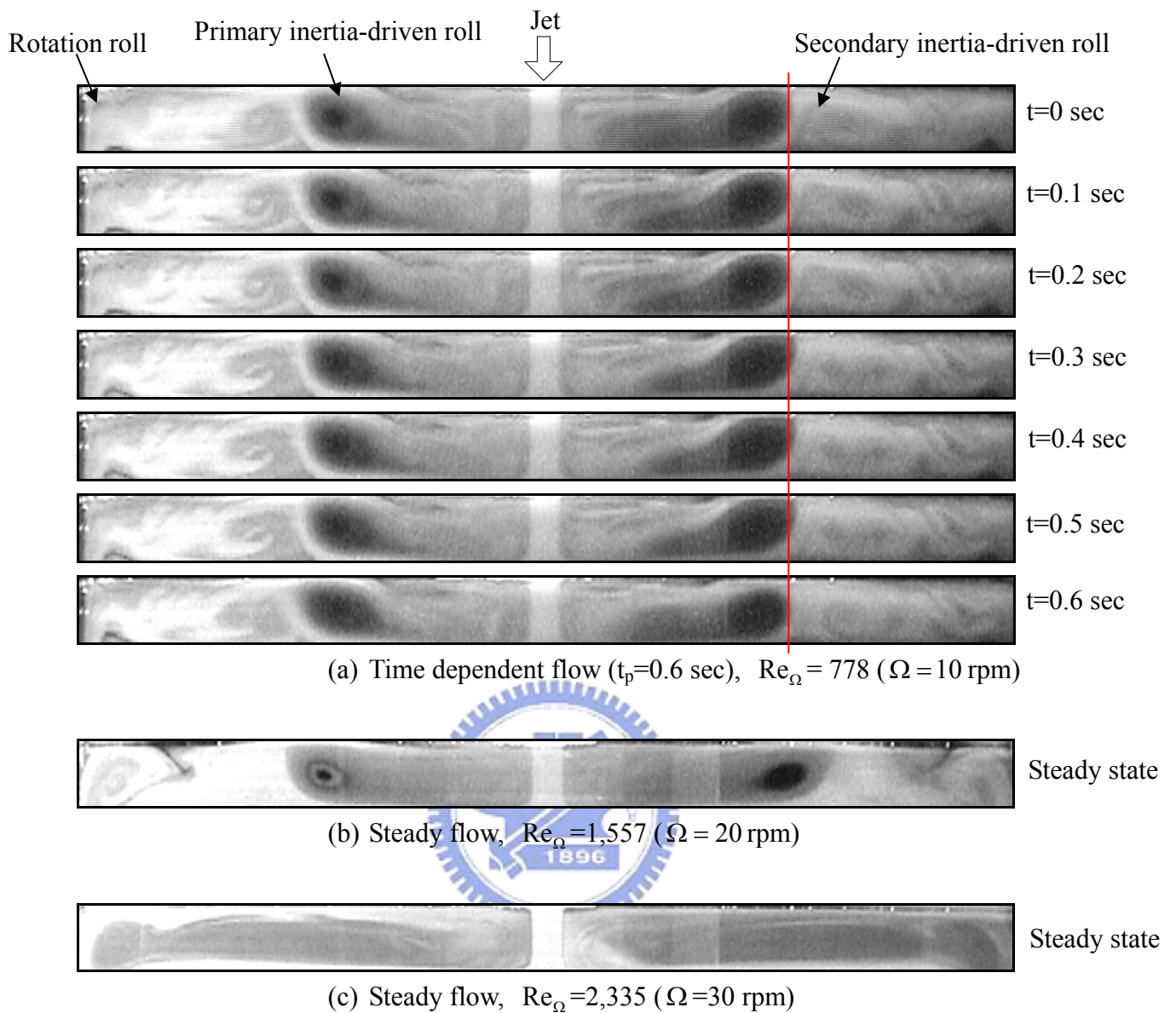


Fig. 4.44 Steady and time-periodic vortex flows for  $H=20.0$  mm and  $Ra=11,270$  ( $\Delta T=15.0$  ) at  $Re_j=933$  ( $Q_j=6.9$  slpm) for (a)  $Re_{\Omega} = 778$  ( $t_p=0.6$  sec), (b)  $Re_{\Omega} = 1,557$  (steady state), and (c)  $Re_{\Omega} = 2,335$  (steady state).